DISCLAIMER

This report was prepared as an account of work sponsored by an agency of the United States Government. Neither the United States Government nor any agency thereof, nor any of their employees, makes any warranty, express or implied, or assumes any legal liability or responsibility for the accuracy, completeness, or usefulness of any information, apparatus, product, or process disclosed, or represents that its use would not infringe privately owned rights. Reference herein to any specific commercial product, process, or service by trade name, trademark, manufacturer, or otherwise does not necessarily constitute or imply its endorsement, recommendation, or favoring by the United States Government or any agency thereof. The views and opinions of authors expressed herein do not necessarily state or reflect those of the United States Government or any agency thereof. Reference herein to any social initiative (including but not limited to Diversity, Equity, and Inclusion (DEI); Community Benefits Plans (CBP); Justice 40; etc.) is made by the Author independent of any current requirement by the United States Government and does not constitute or imply endorsement, recommendation, or support by the United States Government or any agency thereof.

LA-UR-24-25840

Approved for public release; distribution is unlimited.

Title:	Ring Pull Strain Analysis Version 1.1
Author(s):	Beck, Peter Michael Hayne, Mathew Lindsay Saleh, Tarik A. Eftink, Benjamin P.
Intended for:	Report
Issued:	2025-10-09 (rev.1)

Ring Pull Strain Analysis Version 1.1

Nuclear Technology Research and Development

Prepared for
U.S. Department of Energy
Advanced Fuels Campaign
Peter M. Beck, Mathew Hayne, Tarik A. Saleh, Benjamin P. Eftink
Los Alamos National Laboratory
06/10/2024

SUMMARY

This report details an analysis package, Ring Pull Strain Analysis (RPSA), that can be used to present and quantify digital image correlation (DIC) data as it relates to a gaugeless ring pull test. Gaugeless ring pull is a testing technique for mechanical testing of small annular samples, usually cut from a thin-walled tube. DIC data is often necessary for this kind of test because bending moments present on the ring cause a non-uniform strain distribution and localized measurements are necessary. In addition, the annular geometry of a ring lends itself to a polar representation, which is not present with typical DIC analysis methods. RPSA was made to calculate and plot the polar representation of strain from standard pre-processed DIC data of a gaugeless ring pull test. Further analysis can be done on ring pull including a quasi-uniaxial tensile analysis and coating analysis, which are also performed by RPSA. In addition, due to the universality of DIC plotting and ring pull test analysis, RPSA can accommodate a wide variety of tests, though it is tailored for ring pull testing. This report details how RPSA works, including the theory, assumptions, and logic behind the calculations and the structure of the program.

CONTENTS

ACRONYMS

CSV	Comma Separated Variable File
DIC	Digital Image Correlation
RPSA	Ring Pull Strain Analysis
RPCA	Ring Pull Coating Analysis
MOOSE	Multiphysics Object-Oriented Simulation Environment
DICe	Digital Image Correlation engine

VARIABLES

a	non-dimensional radial coordinate
$\varepsilon(r,\theta)$	strain tensor at point (r, θ)
$\varepsilon(a,\theta)$	strain tensor at point (a, θ)
θ	angular coordinate (polar)
θ_{test}	evaluation point for strain
θ_i	indexed angular coordinate to evaluate strain
$\Delta\theta$	step size for angular distribution
i	index variable
n	number of points for smoothing
ξ_i	integer location variable
r	radial coordinate (polar)
$R(\theta)$	rotation matrix
r_M	mandrel radius
r_{in}	inner radius of the ring
r_{out}	outer radius of the ring
σ	standard deviation used for Gaussian distribution
w_i	weight value for weighted mean
x	horizontal coordinate (Cartesian)
x_c	horizontal centroid location
y	vertical coordinate (Cartesian)
y_c	vertical centroid location

RING PULL STRAIN ANALYSIS

1. Introduction

Ring pull testing, also known as ring hoop tension testing, is a test method used to determine material properties in the hoop direction of thin-walled tubes by straining rings. This test consists of a ring mounted against two loading pins or "mandrels," which are pulled apart by a uniaxial, displacement-controlled load frame. A multitude of different ring pull geometries and test setups exist [1,2], including gaugeless ring pull, seen in **Fig. 1**. Gaugeless ring pull testing is primarily used to determine the hoop-direction mechanical properties of a material and has been adapted for several applications including nuclear fuel claddings [3, 4, 5], turbine blades [6] and other aircraft applications [7, 8].

While strength values are often directly pulled from effective stress-strain curves generated during these tests, strain in the material is locally variable due to beam bending of the sample during testing [9], so bulk strain measurements are not an authentic representation of the strain occurring in the material. Recent works have seen the use of digital image correlation (DIC) to measure the localized strain in rings during testing [4, 9, 10]. While DIC provides data on localized strains across the entire area of interest, analysis and reporting of this data is often abstract and qualitative in nature. Sample bending also causes a rigid body rotation in the sample, changing the orientation of the coordinate system as the test proceeds. As a result, the ring coordinate system is often misaligned with the sample geometry, forcing researchers to use equivalent (von Mises) strain instead of reporting the full strain tensor. This occurs both in experimental work with DIC [4, 10], as well as simulations of gaugeless ring pull [4, 5, 7, 10].

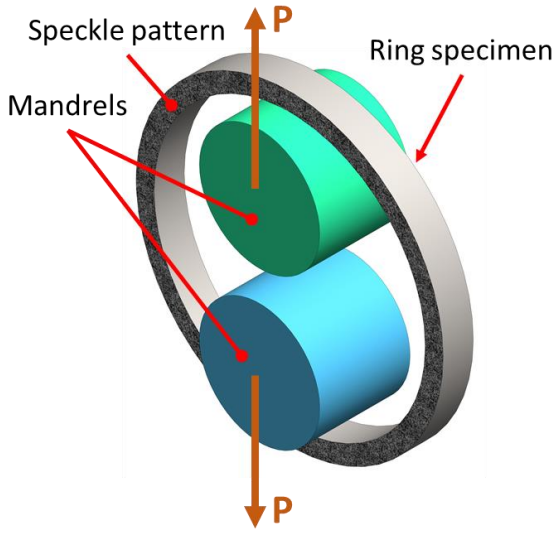

Figure 1. A diagram of the gaugeless ring pull test setup. The force, "P" and the speckle pattern that is required for DIC are displayed in the figure.

There is a need for an analysis procedure that can calculate hoop direction strains and provide a quantitative analysis of strain from DIC and simulations. This report describes a method for analysis of DIC and simulation data and details a Python-based package [11] that was created to perform this analysis. The package, titled Ring Pull Strain Analysis (RPSA), contains several plotting and analysis tools specifically catered to gaugeless ring pull testing.

2. Analysis Procedure

Analysis of ring pull testing requires a few assumptions about the experimental setup. First, this analysis procedure assumes a gaugeless ring pull test is being performed with a 2-dimensional digital image correlation (DIC) setup measuring strain on the flat surface of the ring. It is assumed that the undeformed ring is radially symmetric, such that it has uniform wall thickness and is perfectly circular at the beginning of the test. During testing, the strain is assumed to be uniform across the ring width (cylinder height), such that this is considered a 2-dimensional model system.

There are also a few requirements on the data collected during a test. First, load-displacement data must be taken at all points during the test. This load-displacement data must be synchronized with the images taken for DIC analysis such that each DIC image can be matched with its respective load and displacement value. Additionally, a preprocessing step is required using a digital image correlation software to create a point cloud for each image, exported as a comma separated variable file. Each point cloud must contain cartesian based coordinates, material displacement values, and the strain tensor for all selected subsets calculated by DIC. It is assumed that the full 2-dimensional strain tensor is calculated from these displacements. Of the different strain measures, a Lagrange strain calculation is recommended as it accounts for rigid body rotations, which are discussed in the subsequent paragraph. One last assumption is that the point cloud completely encircles the ring but does not necessarily extend to the edge of the material.

The primary goal behind this analysis is to transform the coordinate system to look specifically at hoop-radial directions in the ring. **Fig. 2** shows two coordinate transformations that need to occur to account for this. The first is a cartesian to polar coordinate transformation. This transformation was achieved by performing a standard coordinate transformation, which is given in **Eq. (1)** and **(2)** below. A tensor rotation must be performed on the strain tensor, which is seen in **Eq. (3)** and **(4)**. Rigid body rotations were accounted for by using the Lagrange strain definition. This strain definition refers to strains as they are in the reference geometry, where the polar coordinate system is aligned with the hoop and radial direction of the tube.

$$r = \sqrt{(x - x_c)^2 + (y - y_c)^2} \tag{1}$$

$$\theta = \tan^{-1}\left(\frac{(y - y_c)}{(x - x_c)}\right) \tag{2}$$

$$R(\theta) = \begin{bmatrix} \cos\theta & -\sin\theta \\ \sin\theta & \cos\theta \end{bmatrix} \tag{3}$$

$$\boldsymbol{\varepsilon}(r,\theta) = R(\theta) * \boldsymbol{\varepsilon}(x,y) * R^T(\theta) \tag{4}$$

Where x and y, and r and θ are the locations of the strain point in cartesian and polar coordinates, respectively, x_c and y_c are the locations of the centroid of the ring, R(θ) is the 2-D rotation matrix, and $\boldsymbol{\varepsilon}(x,y)$ and $\boldsymbol{\varepsilon}(r,\theta)$ are the strain tensor in cartesian and polar coordinates, respectively.

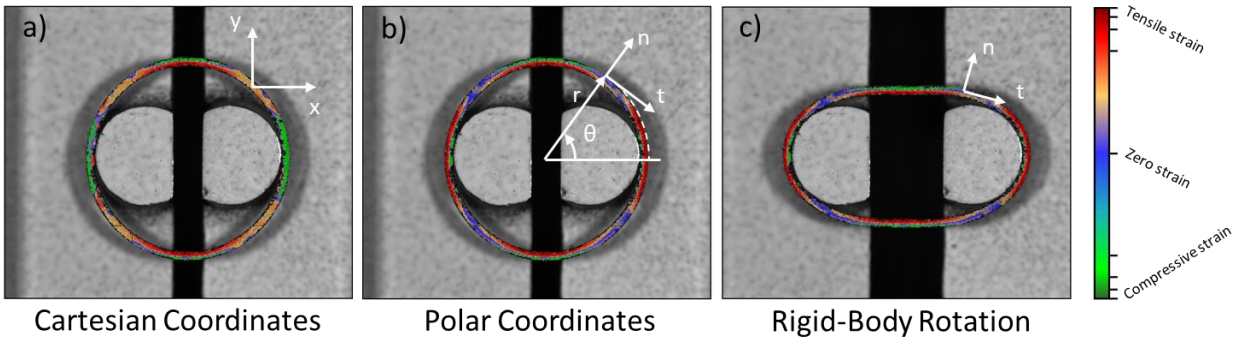

Figure 2. A diagram of a ring with different coordinate systems associated with them: (a) cartesian, (b) polar, and (c) polar with rigid-body rotations. (a) shows strain in the x-direction (ε_{xx}) while (b-c) show strain in the hoop direction ($\varepsilon_{\theta\theta}$).

Due to the annular nature of the ring, one more modification can be made to the coordinate system. The parameter "a" is defined to denote a normalized distance in the radial direction. This parameter is normalized by the thickness, so it is not dependent on the actual dimensions of the ring. Thus, given a well-defined ring geometry, the parameter can substitute the radial coordinate such that (r, θ) → (a, θ) for a particular ring. The transformation is defined in **Eq. 5** and the coordinate system is graphically represented in **Fig. 3**.

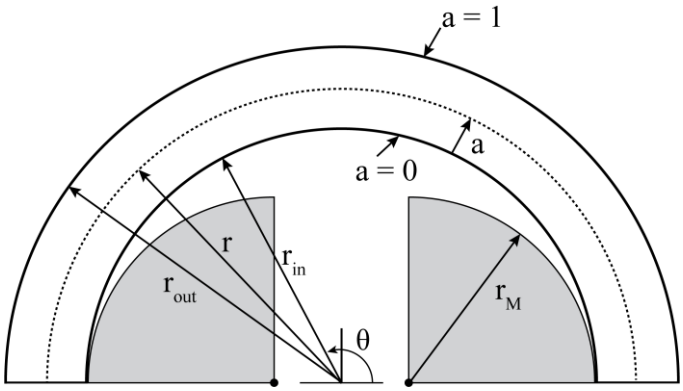

Figure 3. Half-diagram of the ring pull setup. The setup is symmetric about the bottom axis to create a full ring. The parameters r_M, r_{in}, and r_{out} are the mandrel radius, ring inner radius, and ring outer radius.

The parameter "a" is defined as the fraction into the thickness of the ring, where the inner surface corresponds with a = 0 and the outer with a = 1, and r and θ are the coordinates in the polar system

$$r = a * r_{out} + (1 - a) * r_{in} \tag{5}$$

Where r_{in} and r_{out} are the ring inner radius, and ring outer radius and r and a are the radial and "a" parameter coordinate.

After defining the coordinate system and rotating the strain tensor, a strain value can be obtained at any arbitrary location on the ring via mesh interpolation. This mesh is created through use of the quickhull algorithm [12] and then interpolation is performed with a Clough-Tocher scheme [13,14]. This is implemented in SciPy [15]. This interpolation algorithm works when bounded by strain data; however, there is no measurement of strain near the edge of the ring. To approximate the strain value at the edge of the sample, an extrapolation method needs to be employed. Currently, there are no robust 2-D extrapolation methods implemented in SciPy, so a one-dimensional extrapolation is performed that leverages the geometry of the ring. This extrapolation uses interpolated values of strain across the

thickness of the ring. Since the strain is a result of the bending moment acting on the ring, the strain distribution is expected to be linear, allowing prediction of the strain to the edge of the material. There are currently three extrapolation methods available, described here and shown in **Fig. 4**:

(1) An extrapolation line tangent to the interpolated data is considered. This line extends out from the interpolated values. It is sensitive to changes in the slope at the edge DIC values.
(2) A linear regression of the interpolated data is used to extrapolate values outside the range. Previous usage has shown that this method can become erroneous due to values occurring near the inner surface (i.e. at 0 < a < 0.2). As a result, only data at a > 0.5 is used for the regression.
(3) The last interpolated data point is used as the strain at the edge. This method often underestimates the strain; however, it is less sensitive to noise than the other methods.

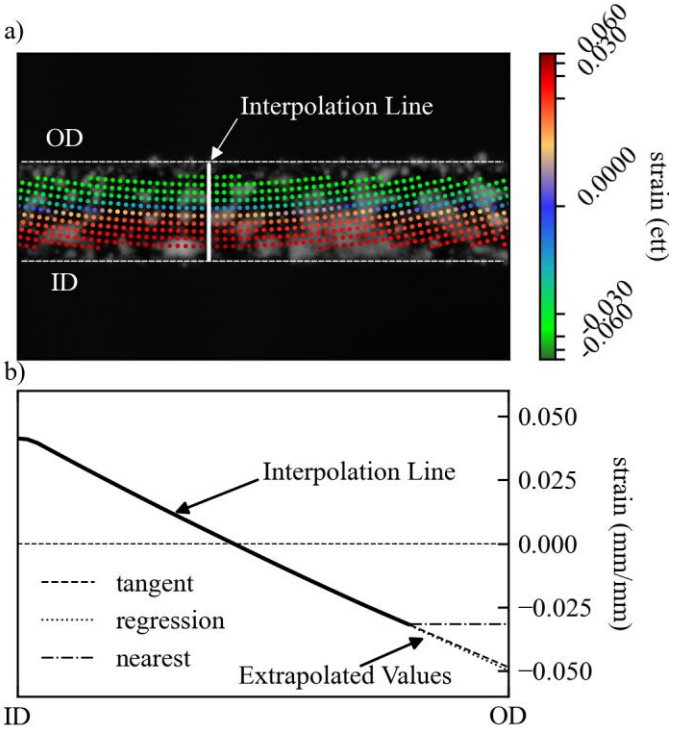

Figure 4. (a) Strain values are interpolated across the thickness of the ring from the DIC data. (b) The interpolated values are then used to extrapolate the line to the edge of the sample. The three possible regression methods are shown in the plot as dashed lines.

Depending on the method, the extrapolation can be sensitive to errors in the data. To mitigate this, a one-dimension Gaussian smoothing filter is applied along an iso-radial curve centered on the point of interest. This smoothing function looks at n = 11 smoothing points evaluation points evenly distributed around the evaluation point, θ_{test}. A location variable, ξ_i is used to denote the integer location away from the center evaluation point and is defined in **Eq. 6**. This location variable corresponds with the angular coordinate, θ_i and is defined in **Eq. 7** using an angular step size of $\Delta\theta = \frac{\pi}{50(n-1)}$. Then a weighted mean (**Eq. 9**) is used to smooth the returned strain value using weights defined by a normalized Gaussian distribution (**Eq. 8**) with a standard deviation of σ = 1.75. The weights, integer location, and angular distance from the center are given in **Table 1**.

$$\xi_i = -floor\left(\frac{n}{2}\right) + i, \quad i \in [0, n] \tag{6}$$

$$\theta_i = \theta_{test} + \xi_i * \Delta\theta \tag{7}$$

$$w_i = \frac{\exp\left(\frac{-1}{2}\frac{\xi_i^{\,2}}{\sigma^2}\right)}{\sum_{i=1}^{n}\exp\left(\frac{-1}{2}\frac{\xi_i^{\,2}}{\sigma^2}\right)} \tag{8}$$

$$\boldsymbol{\varepsilon} = \sum_{i=1}^{n} w_i * \boldsymbol{\varepsilon}(a, \theta_i) \tag{9}$$

Table 1. Weight coefficients and distance from the evaluation point are given corresponding with their respective index.

Index i	Location ξ_i	Angular Distance $\xi_i * \Delta\theta$	Weight w_i
1	-5	-1.80°	0.00385362
2	-4	-1.44°	0.01675005
3	-3	-1.08°	0.05252339
4	-2	-0.72°	0.11881708
5	-1	-0.36°	0.19390747
6	0	0.00°	0.22829677
7	1	0.36°	0.19390747
8	2	0.72°	0.11881708
9	3	1.08°	0.05252339
10	4	1.44°	0.01675005
11	5	1.80°	0.00385362

3. Ring Pull Analysis

The previous section described basic calculations to perform the coordinate system transformation and interpolation and smoothing operations on the data. Once this is done, analysis of gaugeless ring pull tests can be performed. The sections below describe two methods for analysis of ring-pull specific features within a test, named multi-image strain correlation and quasi-uniaxial test analysis.

3.1 Multi-Image Strain Correlation

For tubes with an exterior coating layer on them, performing gaugeless ring pull tests on these rings also stresses the coating layers, and may cause cracks, spallation, and other failure events to occur. These features, if optically visible, could be correlated with loading on the ring to measure the failure stress of this outer layer, similar to coating analyses performed with 4-point bend specimens [16,17]. However, gaugeless ring pull testing involves a complex loading condition on the ring and there are no analytical loading solutions available; instead, DIC could potentially be used to measure the strain during coating failure. However, this is technically difficult for two reasons:

(1) A DIC speckle pattern cannot be placed on the coating to measure the strain; it would cover the coating, making it difficult to see failure. Additionally, for thin coatings, the thickness of the paint is close to the coating thickness, which could change the mechanical properties of the coating.
(2) A stereo-DIC setup would be needed to capture displacements of a rounded surface with out of plane motion. The large out of plane motion that the ring undergoes makes alignment of focus depth regions difficult.

To bypass these problems, the measured strain in the bulk material is combined with the assumption of width-independent strain to measure the failure strain of these coatings. This is made possible by a second camera which images the side of the ring. This camera must share an axis with the DIC camera such that the two images from the respective cameras share either an x-axis or y-axis (or that the x-axis of one corresponds to the y-axis of the other). It is most natural to rotate the camera by 90° but is not strictly necessary to do so.

Features observed on the side of the ring can be correlated to the strain map by calculating the horizontal distance, δ, between the failure and a reference point, usually the mandrel. The distance in pixels is converted to physical distance units using the scale of the image (in mm/pixel). Since the two images share an axis, the distance from the mandrel can be projected onto the strain map as a line, which can be seen in **Fig. 5**. The intersection between the line and a line describing the outer diameter of the ring can then be used to locate the coating failure on the DIC map. Due to the limitations of DIC, the measured strain map does not extend to the edge of the ring and therefore must be calculated using one of the extrapolation methods described in Section 2.

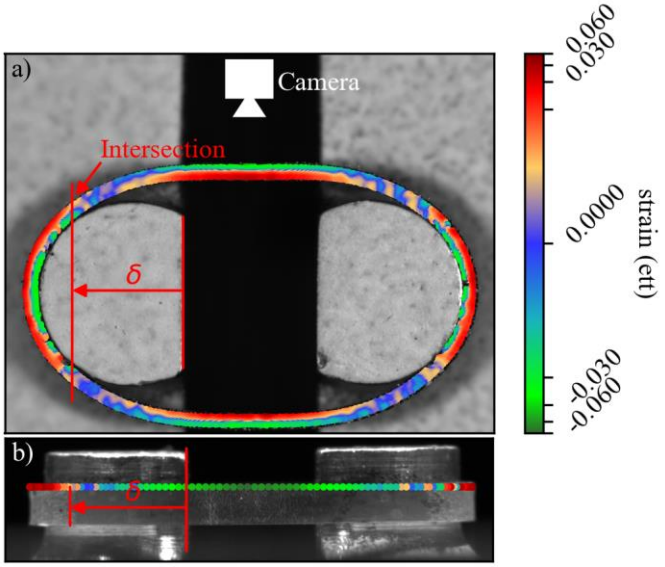

Figure 5. Figure of (a) the DIC strain map along with (b) an image of the side of the ring. The strain on the outer surface is overlayed onto the side of the ring. Annotations of the calculated distance, the intersection point, and the orientation of the side-view camera are shown in the figure.

3.2 Quasi-uniaxial Test Analysis

A common analysis method for Material properties can be obtained from the load-displacement curve by performing an analysis which is analogous to the ASTM E8 standard for analyzing uniaxial tensile tests [18]. With this, several figures of merit can be obtained, including the 0.2% offset strength, ultimate strength, uniform and non-uniform elongation, and total elongation. For this, the load-displacement curve is normalized to an effective stress and strain using Eq. (7) and (8)(8)[3].

$$\hat{P} = \frac{P}{2wt} \tag{7}$$

$$\hat{d} = \frac{\Delta x}{\frac{\pi}{2}\left(d_{ring} - d_{mandrel}\right)} \tag{8}$$

Where $\hat{P}$ is the normalized load, P is the actual load, w and t are the ring width and thickness, $\hat{d}$ is the normalized displacement, Δx is the displacement, and d_{ring} and $d_{mandrel}$ are the diameters of the ring and mandrel, respectively.

An example ring pull curve is shown in **Fig. 6**. As seen in the curve, there is a linear region between approximately 200-550 MPa. A linear regression, shown in black, is fitted and the normalized displacement is shifted such that regression line intersects with the origin. Then, a parallel line is created with an x-offset of 0.2%, shown in red. The location that this red line intersects the normalized load-displacement curve is considered the 0.2% offset strength. Next, the maximum load is considered the ultimate tensile strength, with the corresponding displacement considered the uniform elongation. Finally, the total elongation is taken as the strain at the fracture point of the sample.

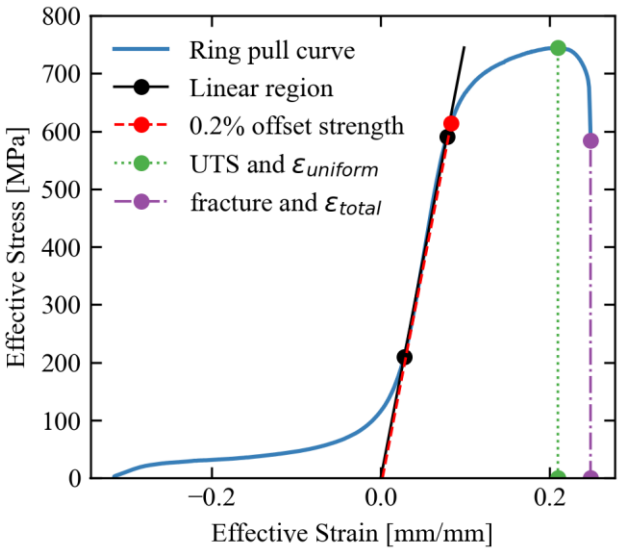

Figure 6. An example of a normalized load-displacement curve from ring pull testing with notations for tensile analysis.

DIC can be used as a digital extensometer to compensate for compliance of the test machine during ring pull. DIC primarily tracks the displacement of individual points, which can be used to calculate the displacement between any two places in the ring. **Fig. 7** shows an image of DIC tracking the points, P_1 and P_2, (defined by the coordinates (a, θ) = (0, 0) and (a, θ) = (0, π)) to get the displacement, $\Delta x = \Delta x_1 + \Delta x_2$, from the initial to the "current" state of the ring. Δx can be as a more accurate measurement to get compliance-corrected displacement values.

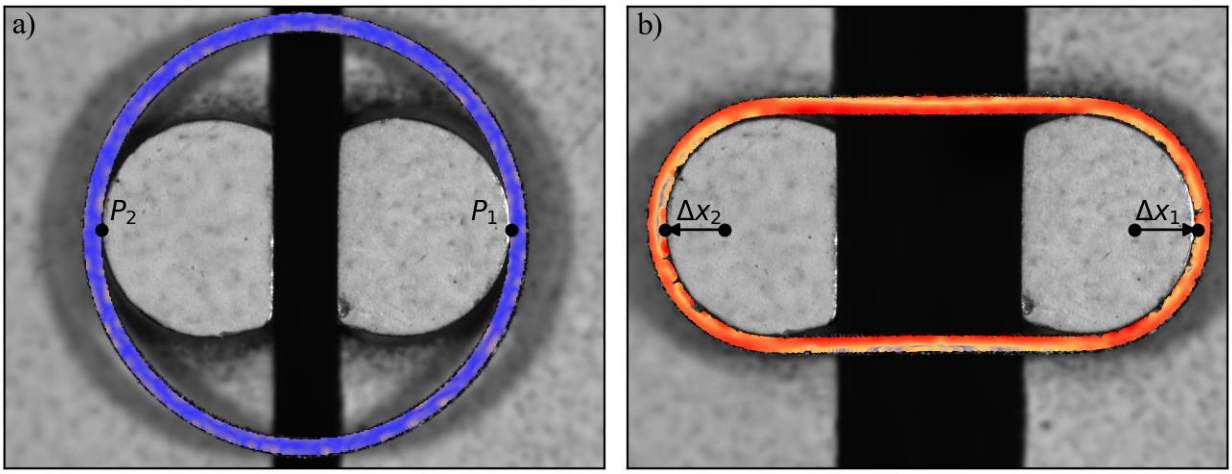

Figure 7. The ring in the (a) reference and (b) deformed position. DIC points close to the mandrel contact point are annotated and show a displacement between the two images.

4. Using Ring Pull Strain Analysis

The Ring Pull Strain Analysis (RPSA) code [11] acts as the implementation of methods described in Sections 2 and 3. RPSA is set up as a downloadable Python module containing two scripts to define functions, classes, and methods for analysis of gaugeless ring samples mechanically tested with DIC.

4.1 RPSA Structure and Inputs

RPSA works by organizing ring pull data into "tests" which are defined by the Python classes ***TensileTest*** and ***RingPull***. The ***TensileTest*** class defines all the methods that perform analysis on uniaxial tensile test data, including methods for calculating 0.2% offset stress, digital extensometers, and plotting methods. This class is primarily intended for analysis of uniaxial tensile tests but can serve as a template for any similar load-displacement curve with DIC data. The daughter class, ***RingPull*** contains all the methods from ***TensileTest***, but also contains methods specific to ring pull testing. Creating a specific instance of one of these classes will fully define a single test, including the load-displacement curve, and corresponding file paths for the DIC images and strain point clouds. These DIC images and point clouds are accessed when the ***TensileTest*** or ***RingPull*** class call the ***TensileImage*** or ***RingImage***, respectively. These two classes define the procedures to compile the raw image and point cloud and they have a plotting method to display the data. As with the ***TensileTest*** and ***RingPull*** classes, ***RingImage*** inherits ***TensileImage*** and adds some additional methods specific for rings, such as the strain tensor rotation, described in Section 2. For analysis of coatings (described in Section 3.1), a separate module is imported to run this calculation. This module, called Ring Pull Coating Analysis (RPCA) is set up as an add on to the RPSA code and is organized in the class, ***RingPullCoatingAnalysis***. This class accepts an instance of the ***RingPull*** class and performs the coating analysis on the defined test. A diagram of the inheritance and calls is displayed in **Fig. 8**.

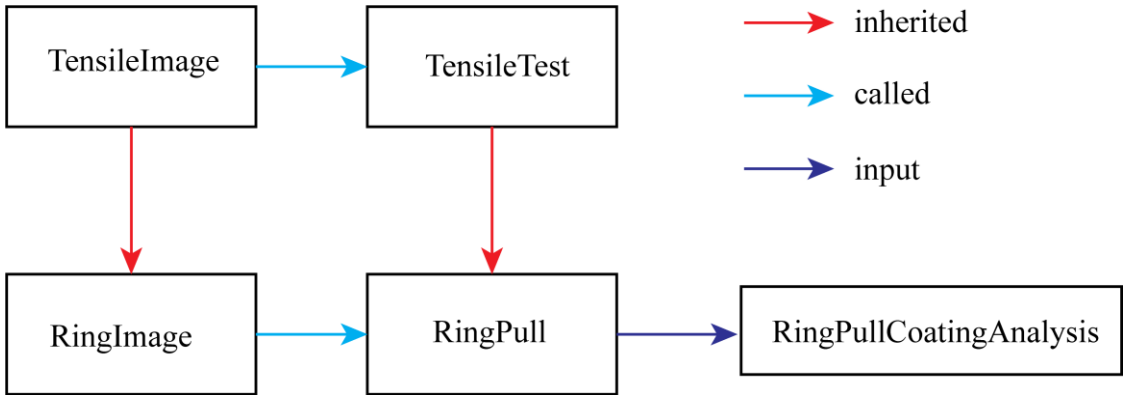

Figure 8. Flow diagram of the classes used in RPSA. The arrows indicate inheritance (red), classes that call other classes (light blue), and classes that take instances of other classes as input (dark blue).

There are a few input datasets required to perform ring pull analysis. First, a comma separated variable (.csv) file containing the load-displacement data from the test is read into the ***TensileTest*** or ***RingPull*** class. This file must have .tiff or .tif image filenames associated with the load and displacement. These filenames, along with corresponding .csv point clouds, are then used to call ***TensileImage*** and ***RingImage***. The .csv point clouds are typically generated by the DIC software or finite element software. Since each software outputs the .csv point cloud column names slightly differently, the program can only take the output of certain software. Currently the module supports file outputs from VIC-2D (Correlated Solutions, Inc.), DICe [19,20] (Sandia National Laboratories), and the modeling software MOOSE [21, 22] (Idaho National Laboratory); however, more software packages can be easily implemented. To perform coating analysis with RPCA, an additional set of images must be added as an extra column to the load-displacement data. This set contains images of the side of the ring that are used to correlate to the top-down strain map. More specifics on data formatting requirements can be found in the Github repository [11].

4.2 Using the module

RPSA is a framework for analysis of ring pull testing. It requires a user to make a separate script calling this module to leverage the previously described analysis techniques. A typical experiment will be performed as follows:

(1) Mechanically test the speckled ring sample, taking images and recording load-displacement data.
(2) If it is not already, correlate the load displacement data with the recorded images.
(3) Perform DIC analysis using a commercial or off-the shelf software. Export the data to .csv files.
(4) Create Python script that imports the collected data using the RPSA framework and run the analysis.

For the creation of an analysis script as described in step (4), there are a few steps that are typically performed:

(1) Call ***RingPull*** class. Here the user specifies geometric parameters of the setup (diameter, thickness, width of the ring, mandrel diameter) and file paths for the load-displacement data taken from the load frame.
(2) Run the ***get_geometry*** function. This allows the program to determine the scale of the image and specify the centroid of the ring based on user-defined concentric circles defining the area of interest on the ring. This function has a user interface (**Fig. 9**(a)) for expedient determination of these circles.
(3) Run analysis. Two analyses of ring pull testing are described in Section 3 and written into RPSA. These also have user interfaces to facilitate expedient operation. The user can create their own analysis as well.

(4) Plot results. This can include plotting the strain maps from specific DIC images (shown in **Fig. 9**(b)), pulling strain values from the images and plotting them, or plotting data from the analysis performed in step (3).

For more specific steps, an analysis script is provided in Appendix A. This script provides some basic analysis using the example ring pull data provided in the repository for this module [11].

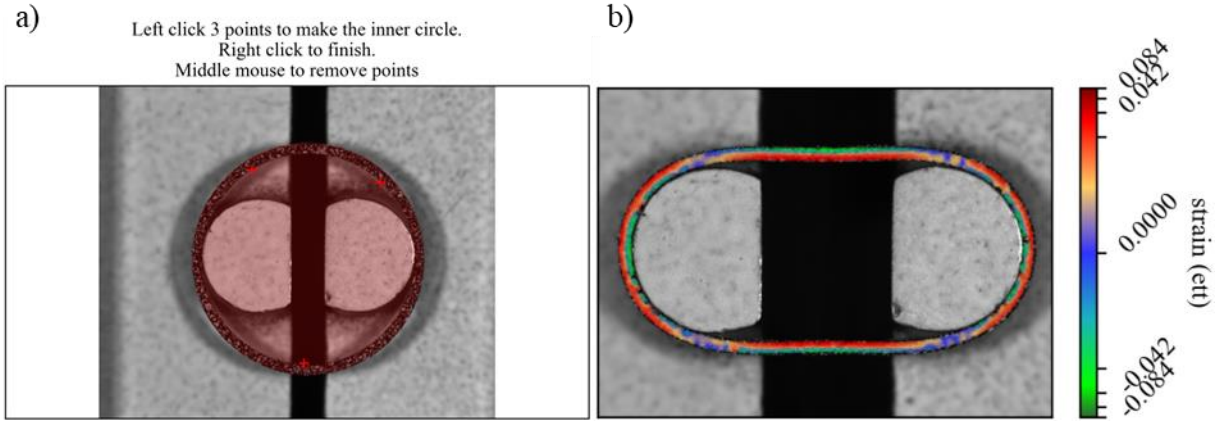

Figure 9. (a) The hoop direction strains are calculated via a user interface to first define the scale and centroid. (b) the strain is then plotted over the original image.

5. Conclusion

Ring Pull Strain Analysis is a Python-based analysis package to analyze localized strains in a sample during testing. This package uses data that was pre-processed by either commercial or open-source digital image correlation software. Hoop strain, which is not readily apparent in DIC output, can be calculated via this program and used as a metric for quantifying strains occurring during gaugeless ring pull tests. Methods for further evaluation of gaugeless ring pull, including evaluation of load-displacement curves and coating failure strain have been described in this report and implemented in the RPSA code.

6. Acknowledgements

This work was supported by the U.S. Department of Energy Advanced Fuels Campaign under DOE Idaho Operations Office and performed at Los Alamos National Laboratory. Los Alamos National Laboratory is an affirmative action/equal opportunity employer, and is operated by Triad National Security, LLC for the National Nuclear Security Administration of U.S. Department of Energy under contract no. 89233218CNA000001. The U.S. Government retains a nonexclusive, paid-up, irrevocable, world-wide license to publish or reproduce the published form of this manuscript, or allow others to do so, for U.S. Government purposes.

7. References

[1] Király, M., Antók, D. M., Horváth, L., & Hózer, Z. (2018). Evaluation of axial and tangential ultimate tensile strength of zirconium cladding tubes. *Nuclear Engineering and Technology*, *50*(3), 425–431. https://doi.org/10.1016/j.net.2018.01.002

[2] Desquines, J., Koss, D. A., Motta, A. T., Cazalis, B., & Petit, M. (2011). The issue of stress state during mechanical tests to assess cladding performance during a reactivity-initiated accident (RIA). *Journal of Nuclear Materials*, *412*(2), 250–267. https://doi.org/10.1016/j.jnucmat.2011.03.015

[3] Yegorova, L., Asmolow, V., Abyshov, G., Malofeev, V., Avvakumov, A., Kaplar, E., Lioutov, K., Shestopalov, A., Bortash, A., Maiorov, L., Mikitiouk, K., Polvanov, V., Smirnov, V., Goryachev, A., Prokhorov, V., Pakhnitz, V., & Vurim, A. (1999). *International Agreement Report Data Base on the Behavior of High Burnup Fuel Rods under Reactivity Accident Conditions*. *2*(July).

[4] Gurovich, B. A., Frolov, A. S., & Fedotov, I. V. (2020). Improved evaluation of ring tensile test ductility applied to neutron irradiated 42XNM tubes in the temperature range of (500–1100)°C. *Nuclear Engineering and Technology*, *52*(6), 1213–1221. https://doi.org/10.1016/j.net.2019.11.019

[5] Youssef, A. (2018). *Influence of Testing Conditions and Thermomechanical Treatments on Tensile Properties of The MYRRHA Cladding By*. *January*.

[6] Hyde, C. J., Hyde, T. H., Sun, W., Nardone, S., & De Bruycker, E. (2013). Small ring testing of a creep resistant material. *Materials Science and Engineering A*, *586*, 358–366. https://doi.org/10.1016/j.msea.2013.07.081

[7] Kazakeviciute, J., Rouse, J. P., De Focatiis, D. S. A., & Hyde, C. J. (2019). The development of a novel technique for small ring specimen tensile testing. *Theoretical and Applied Fracture Mechanics*, *99*(October 2018), 131–139. https://doi.org/10.1016/j.tafmec.2018.11.016

[8] Lavie, W. J., Rouse, J. P., & Hyde, C. J. (2023). The Estimation of Taylor-Quinney Coefficients Using Small Ring Specimens. *Experimental Mechanics*, *63*(3), 429–443. https://doi.org/10.1007/s11340-022-00920-z

[9] Beck, P. M., Hayne, M. L., Liu, C., Valdez, J., Nizolek, T., Briggs, S. A., Maloy, S. A., Saleh, T. A., & Eftink, B. P. (2024). Mandrel diameter effect on ring-pull testing of nuclear fuel cladding. *Journal of Nuclear Materials*, *596*(October 2023), 155087. https://doi.org/10.1016/j.jnucmat.2024.155087

[10] Frolov, A. S., Fedotov, I. V., & Gurovich, B. A. (2021). Evaluation of the true-strength characteristics for isotropic materials using ring tensile test. *Nuclear Engineering and Technology*, *53*(7), 2323–2333. https://doi.org/10.1016/j.net.2021.01.033

[11] Beck, Peter, and USDOE. Ring Pull Strain Analysis. Computer software. https://www.osti.gov//servlets/purl/1907743. USDOE. 16 Nov. 2022. Web. doi:10.11578/dc.20230104.2.

[12] Barber, C. B., Dobkin, D. P. & Huhdanpaa, H. (1996). The Quickhull algorithm for convex hulls. ACM Trans. Math. Softw. 22, 469–483

[13] Alfeld, P. (1984). A trivariate clough-tocher scheme for tetrahedral data. *Computer Aided Geometric Design*, *1*(2), 169–181. https://doi.org/10.1016/0167-8396(84)90029-3

[14] Farin, G. (1986). Triangular Bernstein-Bézier patches. *Computer Aided Geometric Design*, *3*(2), 83–127. https://doi.org/10.1016/0167-8396(86)90016-6

[15] Virtanen, P., et al. (2020). SciPy 1.0: fundamental algorithms for scientific computing in Python. *Nature Methods*, *17*(3), 261–272. https://doi.org/10.1038/s41592-019-0686-2

[16] Hou, P. Y., & Atkinson, A. (1994). Methods of measuring adhesion for thermally grown oxide scales. *Materials at High Temperatures*, *12*(2–3), 119–125. https://doi.org/10.1080/09603409.1994.11689477

[17] Hou, P. Y., & Saunders, S. R. J. (2005). A survey of test methods for scale adhesion measurement. *Materials at High Temperatures*, *22*(1–2), 121–129. https://doi.org/10.1179/mht.2005.014

[18] ASTM International. (2010). ASTM E8/E8M standard test methods for tension testing of metallic materials. *Annual Book of ASTM Standards 4*, *C*, 1–27. https://doi.org/10.1520/E0008

[19] Turner, Dan, Crozier, Paul, Reu, Phil, and USDOE. Digital Image Correlation Engine v.3.0. Computer software. https://www.osti.gov//servlets/purl/1813550. Vers. 3.0. USDOE. 6 Oct. 2015. Web. doi:10.11578/dc.20171025.1658.

[20] Turner, Daniel Z., Crozier, Paul, Reu, Phillip L., and USDOE. Digital Image Correlation Engine v.2.0. Computer software. https://www.osti.gov//servlets/purl/1365551. Vers. v2.0. USDOE. 8 Jun. 2017. Web. doi:10.11578/dc.20220414.51.

[21] Gaston, D. R., Newman, C., Hansen, G., & Lebrun-Grandié, D. (2009). MOOSE: A parallel computational framework for coupled systems of nonlinear equations. *Nuclear Engineering and Design*, *239*(10), 1768–1778. https://doi.org/10.1016/j.nucengdes.2009.05.021

[22] Permann, C. J., Gaston, D. R., Andrš, D., Carlsen, R. W., Kong, F., Lindsay, A. D., Miller, J. M., Peterson, J. W., Slaughter, A. E., Stogner, R. H., & Martineau, R. C. (2020). MOOSE: Enabling massively parallel multiphysics simulation. *SoftwareX*, *11*, 100430. https://doi.org/10.1016/j.softx.2020.100430

APPENDIX A

This appendix contains code for analysis of a gaugeless ring pull test using RPSA. It leverages the data found in the example folder of the GitHub repository [19].

```
## import the necessary modules from the saved folder
import sys
sys.path.insert(0, 'E:\\Projects\\RingPull\\RPSA')
from RingPullStrainAnalysis import RingPull,make_figure
from RingPullCoatingAnalysis import RingPullCoatingAnalysis

##import other important packages
import numpy as np
pi = np.pi
import matplotlib.pyplot as plt
import matplotlib as mpl

## set all the variables needed to run the RingPullStrainAnalysis code:
## the file with the load frame data and their corresponding images
LF_file =
    'E:\\Projects\\RingPull\\RPSA\\RPSA_example\\sample_data\\sample_data_LF.
    csv'
## The DIC analysis software that was used.
DIC_software = 'VIC-2D'
## geometric dimensions of the ring pull test
d_mandrel = 5.1
OD = 10.3
ID = 9.46
W  = 1

## close all other plots that we have created.
plt.close('all')

## create instance of RingPull object
## setting get_geometry_flag to True calls a user interface to determine
## the scale and centroid of the ring
test = RingPull(LF_file=LF_file,
                software=DIC_software,
                ID=ID, OD=OD, d_mandrel=d_mandrel, W=W,
                get_geometry_flag=True)

## use the DIC data to create a digital extensometer on the test sample.
## this will call a user interface to determine the two ends of the
## extensometer.
test.digital_extensometer()

## you can also save the adjusted displacement calculation for future use
test.save_data()

## The complete load-displacement data with calculated stress and strain
## values can be called by looking at the state variable, df
df = test.df

## plot the strain distribution from one of the DIC images
n = 245
```

```
theta = pi/2+1e-4
a = np.linspace(0,1,50)
e = test.open_Image(n).get_value(a,theta,mode='ett', extrap=False)

## RPSA also has a few handy tools to make plotting easier
## such as this make_figure function
f,ax = make_figure()
ax.plot(a,e)
ax.set_xlabel('location on ring (a)')
ax.set_ylabel('strain')


## analyze the curve as if it were a stress strain curve from a tensile test
## and output important material parameters
## can specify the x and y axis to use extensometer or load frame values
E,YS,UTS,eps_u,eps_nu,eps_total,toughness =
    test.process_stress_strain_curve(x_axis='eng_strain')

## plot the effective stress-strain curve
f,ax = test.plot_stress_strain()
ax.set_xlabel('Strain [mm/mm]')
ax.set_ylabel('Stress [MPa]')


## open one of the DIC_image classes from the RingPull object
img = test.open_Image(354)

## again, this data is pulled in from the csv file.
## The object saves it as a DataFrame
df2 = img.df

## Plot the DIC results overlayed on the image
img.plot_Image(state='reference')
img.plot_Image(state='deformed')
## Coordinate transformation is automated and will be performed
## when necessary.
img.plot_Image(state='deformed',mode='ett')

## Create coating analysis instance and run it on a few different frames
method = RingPullCoatingAnalysis(test,mode='compression')
n=[60,65,70]
analysis_data = method.get_side_image_strain(n,debug=False)
```